Reconnection at the Magnetospheric Boundary: Results from Global Magnetohydrodynamic Simulations

Jean Berchem, Joachim Raeder, and Maha Ashour-Abdalla

Institute of Geophysics and Planetary Physics, University of California, Los Angeles

We examine the consequences of magnetic reconnection at the magnetospheric boundary using three-dimensional global magnetohydrodynamic (MHD) simulations of the solar wind interaction with the Earth's magnetosphere. In addition to reproducing the large scale structures expected for steady solar wind conditions, because of the high resolution of the computational mesh used, the simulations show the formation of smaller scale structures at the boundary. In particular we report the formation of magnetic flux ropes at the high-latitude magnetopause for periods with northward interplanetary magnetic field and compare these results with Hawkeye-1 observations.

1. INTRODUCTION

Several three-dimensional (3D) magnetohydrodynamic (MHD) models of the interaction of the solar wind with the Earth's magnetosphere have been developed [*Leboeuf et al.*, 1981; *Wu et al.*, 1981; *Brecht et al.*, 1982; *Ogino*, 1986; *Fedder and Lyon*, 1987; *Watanabe and Sato*, 1990]. While early simulations focused on phenomenological aspects of the interaction, recent global modeling, motivated by the International Solar Terrestrial Physics (ISTP) program, is more quantitative [e.g., *Walker et al.*, 1993; *Raeder et al.*, 1995].

In this paper, we use results from 3D global MHD simulations to examine the consequences of magnetic reconnection at the magnetospheric boundary. Most previous quantitative approaches to these phenomena were based on local models that eluded the local-global duality of the solar wind-magnetosphere-ionosphere interaction. Although some of these models were quite successful in reproducing various aspects of observations and revealed a great deal about local physics [e.g., *Scholer*; *Otto*, this volume], their strong dependency on boundary conditions makes most of them inherently nondeterministic.

A few previous attempts have been made to investigate intermediate scale processes using global MHD simulations. In particular, efforts were made to study the formation of flux transfer events (FTEs) at the dayside magnetospheric boundary for southward interplanetary magnetic field (IMF). These simulations were carried out several years ago, and because of the computing limitations that existed then, severe boundary conditions were imposed to increase the spatial resolution. *Sato et al.* [1986] obtained very good resolution by confining their 3D model to a quarter of the magnetosphere and excluding the nightside and the bow shock regions. Since there was no IMF B_y component in that simulation, twisted magnetic flux tubes were formed by repeated reconnection of the IMF with the Earth's field, first at the subsolar point and then at higher latitudes.

Using 2D global simulations, *Shi et al.* [1988] showed the formation of magnetic islands and suggested that multiple-X line reconnection predominates at the dayside magnetopause because of the high magnetic Reynolds number expected at the boundary. More recently, *Ogino et al.* [1989] carried out 3D simulations for which the IMF had a large B_y component as well as a southward component B_z. They showed that closed field lines earthward of the reconnection region become twisted before they reconnect with the IMF and form magnetic flux ropes that convect tailward across the northern and southern magnetopause. The fine grid (0.5 R_E) used in these simulations was obtained by using a mirror condition at the equatorial plane and including only the near-Earth tail (up

Physics of the Magnetopause
Geophysical Monograph 90

to 25 R_E). Recent advances in computer technology and improvements in numerical techniques allow us to use simulation systems that are not only large enough to properly render the global configuration of the magnetosphere, but also have sufficient spatial resolution to let us investigate mesoscale aspects of magnetic reconnection at the magnetospheric boundary.

In the following sections, after briefly describing our model, we present the global configurations of the dayside magnetosphere obtained with typical solar wind parameters and both southward and northward IMF. We then focus on intermediate scale phenomena by investigating the formation of flux ropes at the high-latitude magnetopause for periods of steady northward IMF and compare these results with spacecraft observations. We conclude this paper by arguing that, in addition to increasing our understanding of the large scale magnetospheric structures, high-resolution global models represent a promising approach to developing a coherent physical interpretation of the formation and dynamics of mesoscale processes.

2. SIMULATION MODEL

Our simulation model is based on the one-fluid MHD description of the interaction between the solar wind and the Earth's magnetosphere. The code solves the resistive MHD equations as an initial value problem [e.g., *Raeder et al.*, 1995]. The algorithm uses an explicit conservative predictor-corrector scheme (accurate to the second order) for time stepping, and fourth-order fluxes hybridized with first-order fluxes for finite spatial differencing. Although diffusion and viscosity appear when the ideal MHD equations are solved numerically, the level of numerical resistivity remains too low to produce the reconnection rates expected at the magnetopause. For this reason we have included a resistive term in Ohm's law, $\mathbf{E} = -\mathbf{v} \times \mathbf{B} + \eta \mathbf{j}$, where the resistivity η is a nonlinear function of the local current density $\mathbf{j}$ such that $\eta = \alpha j^2$, α being a small parameter that is determined empirically. To avoid spurious dissipation we have assumed a threshold that is a function of the local normalized current density. This threshold has been calibrated such that the explicit resistivity is switched on only at a very few grid points in strong current sheets. Similar models have been used in local MHD simulations [e.g., *Sato and Hayashi*, 1979] and are based on the assumption that current driven instabilities are responsible for the anomalous resistivity that produces reconnection.

An inner spherical boundary with a radius of 3.7 R_E is placed around the Earth to exclude the region where the Alfvén velocity becomes too large to allow the use of a reasonable time step. Since this near-Earth region is dominated by the terrestrial field, this procedure does not affect the simulation. Closure of the field aligned currents (FACs) is ensured at every fifth time step by solving self-consistently the ionospheric potential equation:

$$\nabla \cdot \Sigma \cdot \nabla \Phi = -j_{||} \sin\theta$$

where Φ denotes the ionospheric potential, Σ is the tensor of the ionospheric conductance, $j_{||}$ is the FAC at 3.7 R_E mapped onto the polar cap, and θ is the inclination of the magnetic field at the ionosphere. The boundary condition $\Phi = 0$ is applied at the equator. Three ionization sources are then taken into account in computing the height-integrated ionospheric Hall and Pedersen conductivities. The first component is due to solar EUV ionization and is evaluated using *Moen and Brekke's* [1993] model. The second source is constituted by precipitating electrons associated with upward FACs and is computed using the relation established by *Lyons et al.* [1979]. The third contribution comes from diffuse electron precipitation, assuming complete pitch angle scattering of electrons at 3.7 R_E. The conductances are calculated from the precipitation parameters (mean energy and energy flux) using the *Hardy et al.* [1987] empirical relation. The ionospheric potential is then mapped to the 3.7 R_E shell where it is used as a boundary condition for the flow velocity $\mathbf{v} = -\nabla\Phi \times \mathbf{B} / B^2$.

The code has been parallelized for Multiple Instruction Multiple Data machines to allow us to use a large number of grid points ($\approx 1.5\ 10^6$). The dimensions of the system are 23 R_E in the sunward direction (x), 100 R_E along the tail and ± 45 R_E in the y and z directions. Comparison of simulation results using system sizes up to 400 R_E tailward [*Raeder et al.*, 1995] indicates that processes occurring at distances greater than 100 R_E do not significantly affect the dayside magnetospheric boundary. The computational mesh is a stretched Cartesian system and has the highest resolution near the Earth. The grid size varies from 0.4 R_E in a 15 R_E box centered at the Earth to about 7 R_E along the tail axis at $x = -100$ R_E and 2 R_E in the transverse directions at y and $z = \pm 45$ R_E. The simulation box is initially filled with a tenuous ($0.1/cm^3$) and cold (5000°K) plasma. The solar wind magnetic field ($B_z = \pm 5.4$ nT), density ($7.3\ /cm^3$), temperature (65000°K), and velocity (420 km/s) are imposed on the sunward face of the simulation box; open boundary conditions ($\partial/\partial n = 0$) are assumed for all of the other sides of the box.

3. GLOBAL CONFIGURATIONS

Using the set of parameters described above we start the simulation by switching on the solar wind flow with a

southward magnetic field ($B_z = -5.4$ nT) and then let the system evolve. It takes about 40 min for the unphysical initial state to be convected out of the simulation system. At the end of this first stage we obtain an almost stationary magnetosphere for a southward IMF condition with a well formed tail neutral line at about x = −25 R_E. We then instantaneously turn the IMF by 180° at the inflow boundary, and allow the system to evolve for about 30 min. Figure 1 shows the magnetic field lines (top panels), the density contours (middle panels), and the velocity contours (bottom panels) at these two stages of the simulation run. Results for southward and northward IMF are displayed in the left and right panels respectively. Field lines traced in the meridian plane indicate clearly that reconnection with the solar wind takes place in the dayside subsolar region for southward IMF and in the nightside high-latitude region for northward IMF.

From the magnetic field lines and density contours we can identify the different magnetospheric regions. Starting at the left we first see the bow shock, marked by the bending of the IMF lines and the clear jump in density that defines the magnetosheath region. Earthward of the shock, we discern a second boundary separating the high density magnetosheath from the very low density magnetospheric boundary layer. Since the simulation grid size (≈2600 km) in that region remains large as compared to the typical range (400-1000 km) of magnetopause thicknesses, we cannot properly resolve the structure of that transition layer, and thus use a loose definition of the magnetopause to refer to it. Nevertheless, it is clear that the bow shock stand-off and the magnetopause subsolar point distances are found closer to the Earth for southward IMF than for northward IMF and that the flaring of the tail differs significantly between the two cases.

The difference in the shapes of the magnetospheric boundaries is certainly one of the most noticeable global consequences of magnetic reconnection and results from both the transfer of magnetic flux from the dayside to the tail during southward IMF reconnection and its removal from the lobes for northward IMF [e.g., *Aubry et al.*, 1970; *Holzer and Slavin*, 1978]. The subsolar magnetopause location (9.8 R_E) obtained for northward IMF is in fair agreement with the predictions of data based models [e.g., *Petrinec et al.*, 1991; *Fairfield*, this volume] for a similar value of the solar wind dynamic pressure (2.15 nPa). However, for southward IMF we find that the subsolar bow shock and magnetopause are closer to the Earth than predicted by the same models. A plausible explanation for this discrepancy is that the simulated subsolar bow shock and magnetopause shapes appear to be flatter than the shape assumed in the models. Although such a feature has not yet received any observational support, it seems to be a common trait in most of the recent global MHD simulation results for southward IMF.

Another global consequence of magnetic reconnection visible in the density plots shown in Figure 1 (middle panels) result from changes in the cusp magnetic field topology. The simulation shows that closed dayside field lines drape over the cusp during periods of northward IMF. As a result, they close the external cusp region to the direct entry of magnetosheath plasma. For southward IMF, we observe a net accumulation of plasma at the entrance of the magnetic cusp, marked by higher densities and strong gradients. This indentation remains for northward IMF, but at higher latitudes and only in the lower density range, indicating that some magnetosheath plasma might have been trapped in the process or is penetrating into that region. Most of this plasma is now on closed field lines. In contrast, the high density region of the magnetosheath appears as a relatively smooth layer between the bow shock and the magnetopause. This layer is also thinner and more dilute than for southward IMF field. In addition, the magnetopause region seems more diffuse, making it reminiscent of the formation of a depletion layer [*Zwan and Wolf*, 1976]. However, since the thicknesses of the depletion layer observed for northward IMF [e.g., *Phan*, this volume] are at most of the order of the grid size used here, higher spatial resolution is required to resolve that layer accurately.

The bottom panels of Figure 1 show contours of the north-south component of the plasma velocity (v_z). We limited the range of velocities to ±140 km/s so that low contours can be distinguished. Since locally accelerated flows are expected to be present in the reconnection region [e.g., *Lee*, this volume], it is interesting to compare the global simulation results for both southward and northward IMF orientations. Looking first at the magnetosheath layer close to the shock we observe that the flow contours are very similar to those obtained by early gas-dynamics simulations [*Spreiter et al.*, 1966]. Nevertheless, the low velocities observed far from the sun-Earth axis for southward IMF reveal that the subsolar region of that layer is affected by the reconnection process occurring at the magnetopause. These low velocities are consistent with the high densities noted above and may result from a less efficient squeezing of the entire subsolar magnetosheath than the one observed for northward IMF. Recent superposed epoch analysis of the plasma parameters and the magnetic field for the magnetosheath region adjacent to the dayside magnetopause shows that the average flow tangential to the boundary for high-shear magnetopauses (100 km/s) is slower than for low-shear magnetopauses (150 km/s) [*Phan*

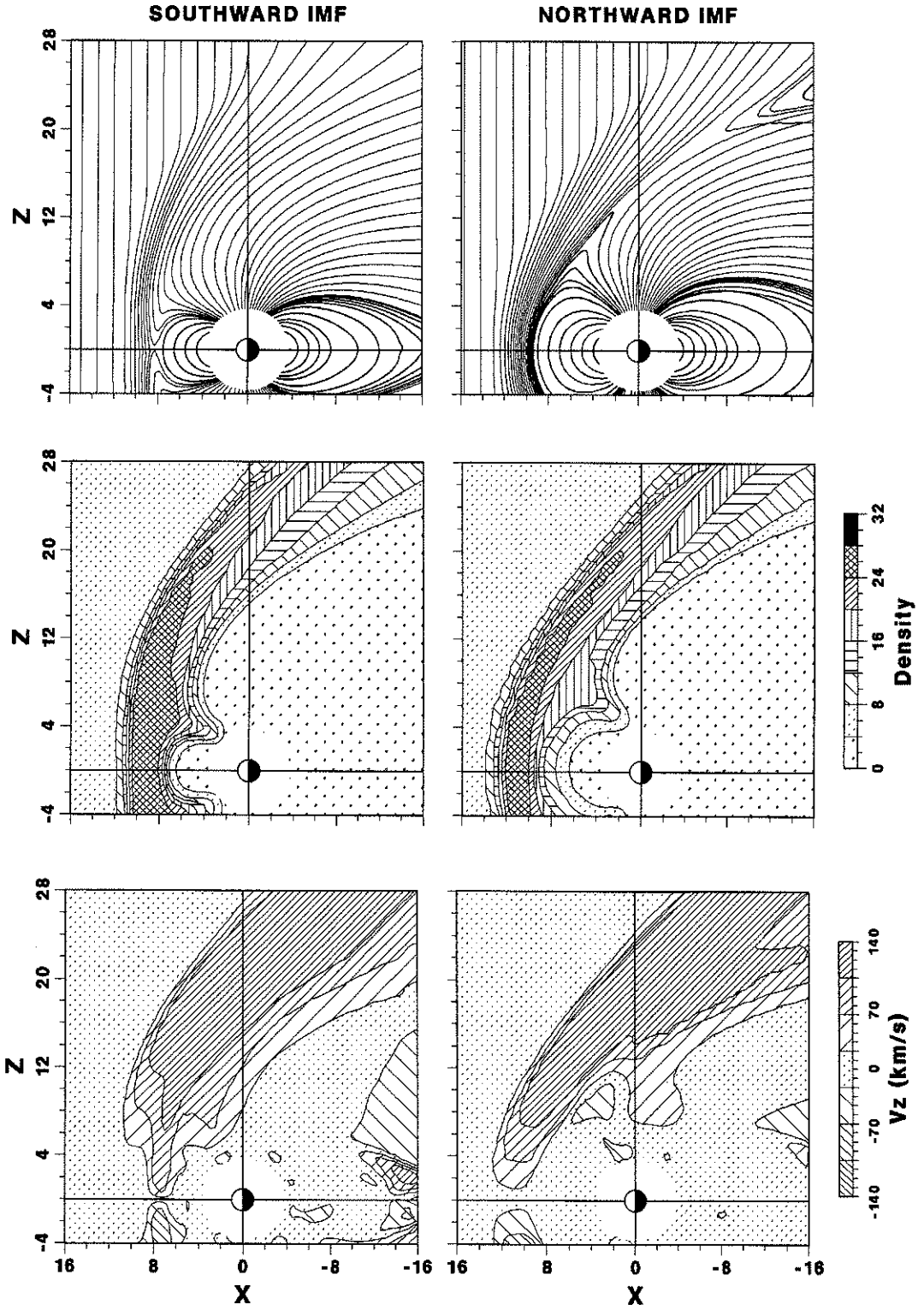

Fig. 1 Dusk view of the meridian plane for southward (left panels) and northward (right panels) IMF showing magnetic field lines (top panels), contours of the plasma density in cm^{-3} (middle panels), and contours of the northward component of the velocity in km/s (bottom panels); the magnitude of the IMF is 5.4 nT and the dynamic pressure of the solar wind is 2.15 nPa, distances are in units of the Earth's equatorial radius (1 R_E = 6378 km).

et al., 1994]. Although the authors attribute this effect to different causes, these observations seem consistent with the low subsolar magnetosheath velocities seen in our results for southward IMF.

Closer to the magnetospheric boundary, flow contours radically diverge from the contours that are expected to form around a blunt obstacle. For southward IMF, the accelerated flows produced by magnetic reconnection in the subsolar magnetopause region are clearly evident. They are directed northward ($v_z > 0$) above the sun-Earth axis and southward ($v_z < 0$) below it. Tailward of the cusp and earthward of the magnetopause, we also see the formation of the plasma mantle characterized by high plasma velocities. This layer results from the rapid tailward expansion of the plasma eroded from the dayside along the newly reconnected field lines. Accelerated plasma flows resulting from magnetic reconnection for northward IMF are also observed, but in the high-latitude magnetopause region. Although tailward flows are difficult to distinguish from the high speed magnetosheath flow, a clear indentation in the velocity contours tailward of the reconnection region ($v_z > 0$) and fast counter-streaming plasma flows ($v_z < 0$) sunward of the terminator unambiguously indicate the occurrence of reconnection in that region.

4. MAGNETIC FLUX ROPES

The three panels shown in Figure 2 are snapshots of the magnetospheric configurations taken every 10 min after the IMF has been turned from southward to northward. The display format of these field line plots is identical to that used in Figure 1, i.e., the meridian plane is viewed from dusk. The first snapshot (Figure 2a), taken 10 min after the IMF turning, shows that reconnection is taking place at the immediate tailward edge of the polar cusp. Since the IMF is imposed at the sunward boundary of the simulation system ($x = 23R_E$) it takes at least 4 to 5 min for the discontinuity to reach the subsolar magnetopause. Thus the reconnection process has started at most 5 min before this snapshot is taken. Open field lines of the northern lobe have started to reconnect with magnetosheath field lines, whereas those tailward of the reconnection site have become unconnected, resulting in the erosion of the plasma mantle.

While some field lines cuspward of the reconnection site are still open ended, their new ends are now located in the southern hemisphere. However, since a symmetrical reconnection process is occurring simultaneously in the southern hemisphere, most of these newly opened lines reconnect there too and form new closed field lines. As a

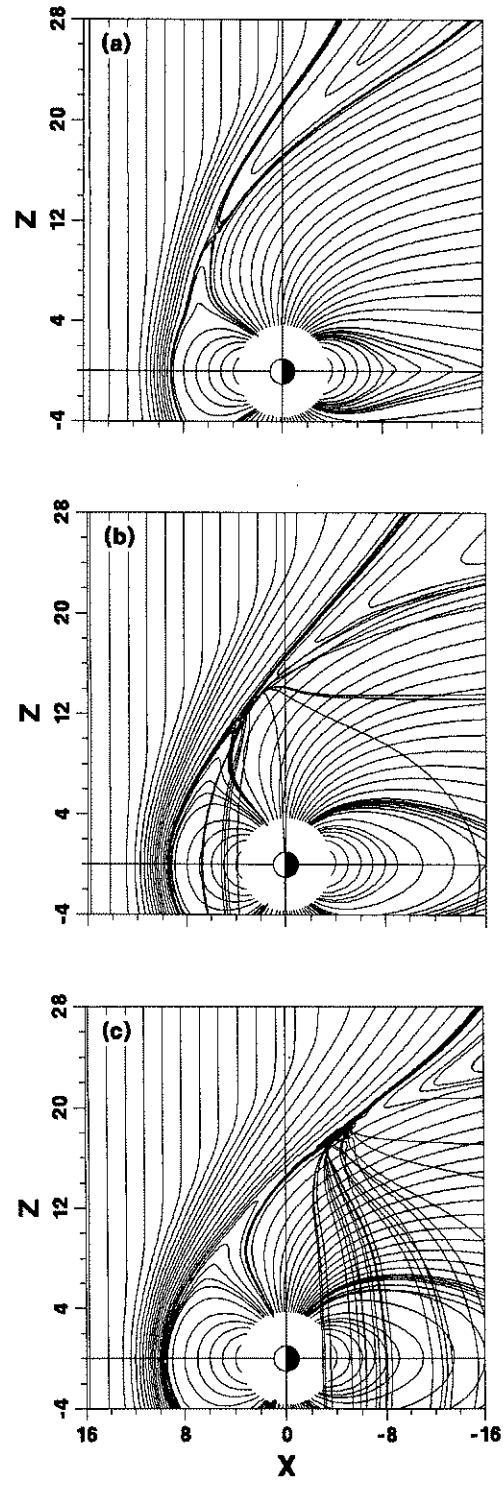

Fig. 2 Dusk views of the meridian plane showing magnetic field lines traced at different times of the simulation. Panels (a), (b), and (c) show the magnetic field configurations obtained at 10, 20 and 30 min, respectively after the northward turning of the IMF at the upstream boundary located at x = 23 R_E.

result, the magnetopause moves sunward, and the flaring of the near-Earth tail decreases. This process is readily seen in the second snapshot (Figure 2b) taken 10 min later, i.e., 20 min after the northward turning. In the elapsed time the subsolar magnetopause has moved sunward by 0.5 R_E, while the reconnection site has moved by about 1 R_E northward and 3 R_E tailward, increasing the amount of the dayside magnetic flux on closed field lines. The small "horn" formed by the newly closed field lines below the reconnection site is now well developed, and the surface of the magnetopause appears fairly smooth. A few open field lines are draping the entire dayside; they are magnetosheath field lines that have reconnected in the southern hemisphere but not in the northern one. Looking closely at the reconnection site seen in Figure 2b, we observe the formation of a small "island" structure to which open and closed field lines are connected in a different order than was seen before. We will show below that these structures are three-dimensional and that these field lines extend out of the meridian plane. The open field lines are convecting around the magnetosphere and slipping on the magnetospheric boundary, whereas the closed field lines are part of the flank boundary itself.

In the next snapshot (Figure 2c) taken 30 min after the northward turning, we notice that the subsolar location of the last closed field line has remained unchanged. However, the reconnection site has moved significantly and is now located on the nightside. As a result, closed dayside field lines are stretched toward the nightside, recovering the cusp region and forming an elongated current sheet above most of the polar region. A very similar magnetic field topology was reported by *Wu* [1985]. The "island" structure at the reconnection site has grown and the field lines out of the plane have moved to the nightside. These field lines bend tailward because they convect faster along the magnetospheric flanks than the reconnection site. By this time, the reconnection site has reached a stationary location, as plots for the next time steps (not shown here) indicate.

A three-dimensional rendering of the northern magnetosphere viewed from the duskside at about 17:00 local time is displayed in Figure 3. It shows that the ropes in the high latitude nightside region are draping over the magnetospheric flanks. The other detached field lines seen on the front side are in the process of being draped over the dayside, and are now slipping on the dawn magnetospheric boundary but are not connected to the northern reconnection site. A complete mapping of these field lines (not shown here) indicates that they are the southern counterpart of those seen on the nightside.

Close-up views of the tip of the current sheet seen in Figure 2c are displayed in Figure 4. A view from dusk

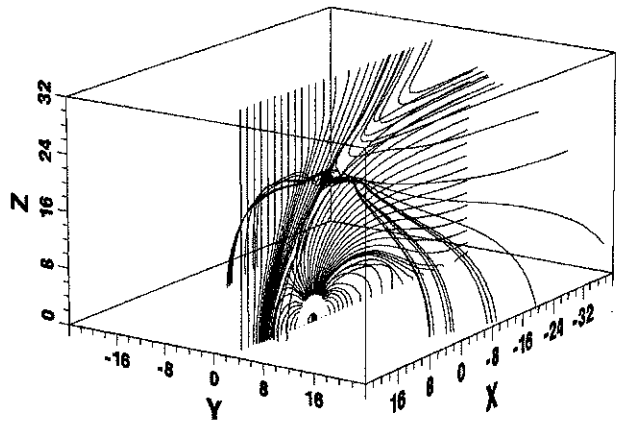

Fig. 3 Three-dimensional plot of the magnetic field lines shown in Figure 2c. The northern magnetosphere is viewed from the afternoon sector; only field lines originating from the dusk side of the meridian plane are plotted.

(Figure 4a) shows that the overall island structure is wedge shaped. It lies between closed field lines and a mixture of magnetosheath field lines and southern open field lines. The whole structure extends over at least five cells of the computational mesh, and is about 2 R_E long and almost 1 R_E thick. However, a view from the sun (Figure 4b) reveals that the island structure seen in Figure 4a results from an artifact of the orthogonal projection. The field lines extending out of the meridian plane have helical structures that are characteristic of twisted magnetic field tubes or magnetic flux ropes.

It is interesting to note that the ropes are formed by the intertwining of both open and closed field lines that are stretched over the polar region. As a consequence, each rope has at least one end attached to the Earth, and since these ends are located in the meridian plane, the ropes do not cross the meridian region. Two distinct systems of ropes are thus formed dawnward and duskward of the meridian plane, depending on the side of the magnetospheric boundary on which the equatorial portion of the ropes are convecting. This feature is readily seen in Figure 4b and leads to dawn and dusk ropes having opposite helicity, since the field reverses its direction at the meridian plane.

As we will see below the plane of symmetry of the two systems lies along the direction of the IMF and is thus the meridian plane for the purely northward IMF case shown here. The slight duskward offset ($\approx 0.5\ R_E$) of the plane of symmetry seen in Figure 4b results from the day-night gradient in the ionospheric Hall conductance that rotates the polar cap convective flow [e.g., *Atkinson and Hutchinson*, 1978]. The mixture of open and closed field lines is

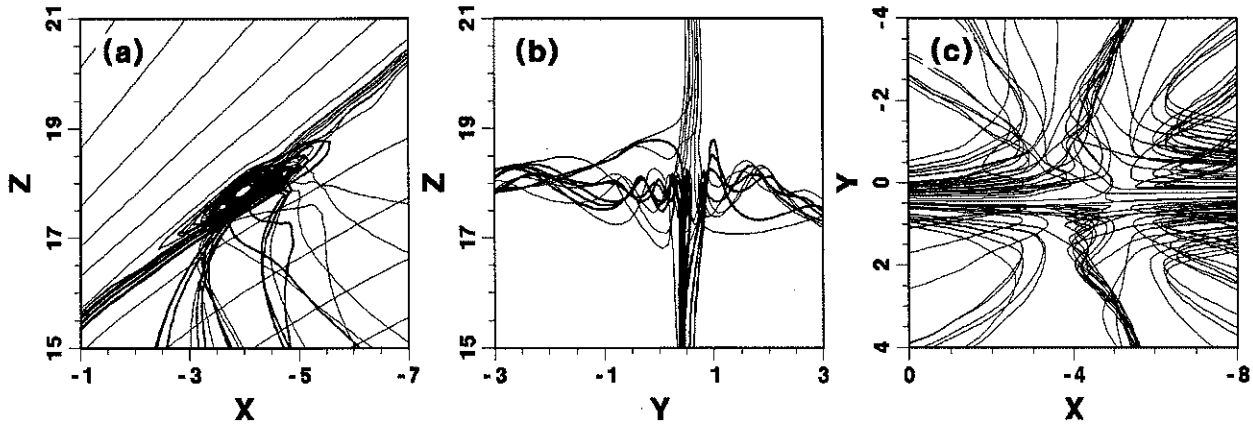

Fig. 4 Close-up views of the reconnection site and the magnetic flux ropes. Two-dimensional projections of the magnetic field lines in the x-z (a) and y-z (b) planes are viewed from dusk and noon respectively. Panel (c) is a view from above the reconnection site, the sunward direction being on the left.

important since it suggests that the plasma composition found in these flux tubes is a mixture of magnetosheath and magnetospheric plasma.

Most of the properties mentioned above are reminiscent of the FTEs observed at the dayside magnetopause [e.g., *Elphic*, this volume] and give us clues that help account for the rope formation. In looking down at the reconnection region along the z axis (Figure 4c), we observe a magnetic field topology very similar to that proposed by *Lee and Fu* [1985] to explain the formation of FTEs. They suggested that the presence of a B_y component in the magnetosheath field leads to multiple interconnections with the geomagnetic field lines and hence to the formation of twisted field lines between merging lines. The only difference between Lee and Fu's reconnection geometry and that seen in Figure 4c is that in Figure 4c multiple reconnections occur independently on each side of the meridian plane, leading to the formation of two sets of ropes as seen in Figure 4b. A significant new feature is that the component transverse to the geomagnetic field, which is needed to produce magnetic flux ropes, is not imposed by the east-west component of the IMF, but results from the convection and draping of the magnetic field lines along the magnetospheric boundary. As a consequence, the east-west component of the IMF does not control the process, which explains why the ropes occur even for purely northward IMF. This result was confirmed by running a simulation (not shown here) where the IMF was rotated by a 30° clock angle. In that simulation, magnetic flux ropes are also observed, but they are formed away from the meridian plane and closer to the plane lying along the IMF direction.

5. OBSERVATIONS

In order to test the validity of the ropes found in our simulations, we surveyed early Hawkeye-1 measurements from the onboard magnetometer [*Van Allen et al.*, 1974]. With an initial apogee of about 21 R_E and an inclination relative to the equator of approximately 90°, Hawkeye-1 provides broad coverage of the high-latitude magnetopause [e.g., *Van Allen and Adnan*, 1992]. Since we expect that the ropes are well developed predominantly in the nightside region, we limited our search to observations near midnight magnetic local time (MLT). In addition, we used IMP 8 solar wind data to select magnetopause crossings for which the IMF was predominantly northward for at least 1 hour previous to the crossings. This selection procedure left us with a very small data set, about 25 events, from which 5 exhibited the spiky signatures to be expected when such rope structures are crossed. Figure 5 shows one of these crossings. In that figure, Hawkeye-1 magnetic field measurements from 12:00 UT to 13:00 UT on November 25, 1974, are plotted using 5.76 second resolution data that we averaged over 3 samples and then overlapped by 2/3 to restrict the bandwidth. The data are rotated in boundary normal coordinates (**l**, **m**, **n**) as defined by *Russell and Elphic* [1978]; the direction normal to the magnetopause (**n** = 0.329, 0.321, 0.867 in GSM coordinates) was calculated using the cross product of the average magnetospheric and magnetosheath field vectors. Looking at the total magnetic field we can identify three crossings of the magnetopause at 12:40, 12:46, and 12:47 UT. At the time of the first crossing the spacecraft was located at about 80° in dipole

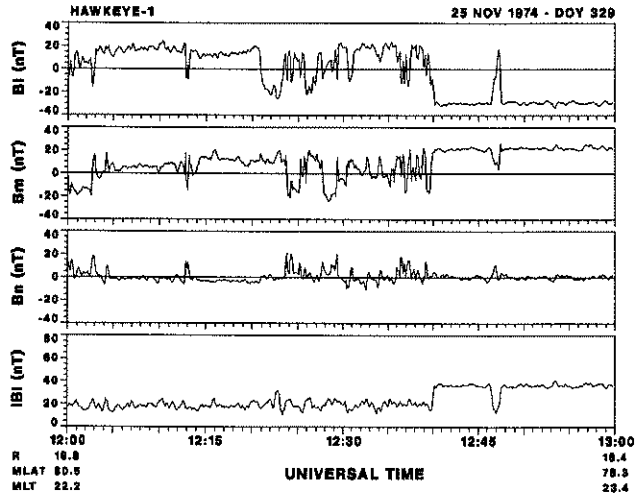

Fig. 5 Magnetopause crossings observed by the Hawkeye-1 spacecraft on November 25, 1974 (Day Of Year = 329). The data are plotted in boundary normal coordinates; R indicates the radial geocentric distance of the spacecraft in units of the Earth's equatorial radius; MLAT is the dipole magnetic latitude and MLT is the magnetic local time in hours.

magnetic latitude (MLAT) and 22.2 hours MLT. On this inbound pass, we observe a fairly constant average field magnitude (≈20 nT) before the first magnetopause crossing, indicating that we are plausibly in the magnetosheath field for the entire time prior to 12:40 UT. This identification is partially confirmed by looking at the l component of the field (l points roughly northward and tailward) as it shows the orientations of the field measured from 12:05 to 12:20 UT, and the one from 12:40 to 13:00 UT to be very distinct (except for the small incursion into the sheath field around 12:47 UT). Between those two periods (from around 12:25 to 12:35 UT) we observe a greatly fluctuating field marked by the occurrence of several bipolar signatures in the normal component and a field direction that has neither of the orientations previously identified. In addition, a small bipolar signature accompanied by a small increase in the total field is observed in the magnetospheric field around 12:53 UT. These features are fairly consistent with the signatures that one would expect when crossing the ropes seen in the simulations. The somewhat weak increase in the field magnitude observed during these events might indicate that we are relatively far from the reconnection region. More obtrusive and better defined events may be found when a more systematic search of the Hawkeye-1 data is undertaken. On the other hand, the signatures observed here may be due to other processes occurring at the magnetospheric boundary, and plasma measurement must be used to confirm that they result from the crossing of magnetic flux ropes.

Earlier Heos-2 data sets might provide additional clues for the occurrence of the magnetic flux ropes. *Haerendel et al.* [1978] identified spikes on the magnetospheric side of the high latitude magnetopause that they interpreted as events of impulsive erosion of magnetic flux tubes. As *Rijnbeek and Cowley* [1984] demonstrated later, these events are identical to the FTEs identified by *Russell and Elphic* [1978] at lower latitudes. Since the ropes observed in the simulations start forming in the dayside cusp (Figure 2b), it is possible that some impulsive events reported by *Haerendel et al.* [1978] might have been caused by such structures passing over the spacecraft.

6. DISCUSSION AND CONCLUSIONS

The simulation results shown in this paper are only a few examples of the large and intermediate scale consequences of reconnection at the magnetospheric boundary that now can be addressed because of improvements in our global MHD simulations. It is thus important to discuss the validity of such an approach. Clearly, our model has the basic limitations inherent in the single fluid MHD description and thus assumes a constant polytropic index and neglects consideration of the identity of individual particles. These limitations preclude the description of important phenomena such as the presence of anisotropic plasmas or the growth of microscopic instabilities; hence it is obvious that our simulation model cannot render some of the plasma properties observed in the magnetosheath [see *Phan*, this volume], resolve the fine structure of the boundary [see *Russell*, this volume], or reproduce the microphysics involved in the reconnection process [see *Drake*, this volume]. The self-consistent global 3D particle models needed to resolve these microscopic processes are far beyond our present computing capability. However, we believe that high resolution global MHD models can contribute significantly to our understanding of the formation and dynamics of intermediate scale processes such as the formation of the ropes reported in the present study.

Of course, the central issue in global modeling remains the control of the dissipation producing reconnection. Although our present model is far from optimal, its low numerical dissipation has permitted us to include phenomenological models that could produce the local resistivity expected from current driven instabilities and refine the description of the ionospheric boundary. The process of adjusting the different parameters of these phenomenological models, such as the local current threshold of the resistivity, remains empirical and thus subject to caution.

The situation is in fact similar to the one encountered when carrying out local kinetic simulations. Self-consistent particle simulations can reproduce fairly well microphysical processes but do not render the physical processes that control the boundaries of the system, and thus arbitrary boundary conditions have to be imposed on the simulations. On the other hand, in global MHD modeling we have reached the stage where we can control fairly well the boundary conditions of the simulations but encounter difficulties in rendering the physics of the local processes. It is obvious that a convergence of the two approaches is required to yield a satisfactory representation of the physical processes that will ultimately allow the development of accurate predictions of magnetospheric phenomena. Since global self-consistent kinetic simulations are still beyond present computing capacity, using phenomenological models to include more physical processes in global MHD simulations appears, at the present time, to be one of the most effective methods to reach this goal.

Acknowledgments. The authors thank Tomik Ebrahimian and Rebecca McAlexander for their help in developing the visualization software and in reducing the magnetic field data. Computations were performed on the Paragon at the San Diego Supercomputer Center. Funding was provided by NASA ISTP grant NAG5-1100; IGPP-UCLA publication 4200.

REFERENCES

Aubry, M. P., M. G. Kivelson, and C. T. Russell, Inward motion of the magnetopause before a substorm, *J. Geophys. Res.*, *75*, 7018, 1970.

Atkinson, G., and D. Hutchinson, Effect of the day night conductivity on polar cap convective flow, *J. Geophys. Res.*, *83*, 725, 1978.

Brecht, S. H., J. G. Lyon, J. A. Fedder, and K. Hain, A time dependent three dimensional simulation of the Earth's magnetosphere, *J. Geophys. Res.*, *87*, 6082, 1982.

Fedder, J. A., and J. G. Lyon, The solar wind-magnetosphere-ionosphere current voltage relationship, *Geophys. Res. Lett.*, *14*, 880, 1987.

Haerendel, G., G. Paschmann, N. Sckopke, and H. Rosenbauer, The front side boundary layer of the magnetosphere and the problem of reconnection, *J. Geophys. Res.*, *83*, 3195, 1978.

Hardy, D. A., M. S. Gussenhoven, R. Raistrick, and W. J. McNeil, Statistical and functional representations of the pattern of auroral energy flux, number flux, and conductivity, *J. Geophys. Res.*, *92*, 1,275, 1987.

Holzer, R. E., and J. A. Slavin, Magnetic flux transfer associated with expansions and contractions of the dayside magnetosphere, *J. Geophys. Res.*, *83*, 3831, 1978.

Leboeuf, J. N., T. Tajima, C. F. Kennel, and J. M. Dawson, Global simulation of the three-dimensional magnetosphere, *Geophys. Res. Lett.*, *8*, 257, 1981.

Lee, L. C., and Z. F. Fu, A theory of magnetic flux transfer at the Earth's magnetopause, *Geophys. Res. Lett.*, *12*, 105, 1985.

Lyons, L. R., D. S. Evans, and R. Lundin, An observed relationbetween magnetic field aligned electric fields and downward electron energy fluxes in the vicinity of auroral forms, *J. Geophys. Res.*, *84*, 457, 1979.

Moen, J., and A. Brekke, The solar flux influence on quiet time conductances in the auroral ionosphere, *Geophys. Res. Lett.*, *20*, 971, 1993.

Ogino, T., A three-dimensional MHD simulation of the interaction of the solar wind with the Earth's magnetosphere: the generation of field aligned currents, *J. Geophys. Res.*, *91*, 6791, 1986.

Ogino, T., R. J. Walker, and M. Ashour-Abdalla, A magneto-hydrodynamic simulation of the formation of magnetic flux tubes at the Earth's dayside magnetopause, *Geophys. Res. Lett.*, *16*, 155, 1989.

Petrinec, S., P. Song, and C. T. Russell, Solar cycle variations in the size and shape of the magnetopause, *J. Geophys. Res.*, *96*, 7893, 1991.

Phan, T. D., G. Paschmann, W. Baumjohann, and N. Sckopke, The magnetosheath region adjacent to the dayside magnetopause: AMPTE/IRM observations, *J. Geophys. Res.*, *99*, 121, 1994.

Raeder, J., R. J. Walker, and M. Ashour-Abdalla, The structure of the distant geomagnetic tail during long periods of northward IMF, *Geophys. Res. Lett.*, 222, 349, 1995.

Rijnbeek, R. P., and S. W. H. Cowley, Magnetospheric flux erosion events are flux transfer events, *Nature*, *390*, 135, 1984.

Russell, C. T., and R. C. Elphic, Initial ISEE magnetometer results: Magnetopause observations, *Space Sci. Rev.*, 22, 681, 1978.

Sato, T., and T. Hayashi, Externally driven magnetic reconnection as a powerful magnetic energy converter, *Phys. Fluids*, *22*, 1189, 1979.

Sato, T., T. Shimada, M. Tanaka, T. Hayashi, and K. Watanabe, Formation of field twisting flux tubes on the magnetopause and solar wind particle entry into the magnetosphere, *Geophys. Res. Lett.*, *13*, 801, 1986.

Shi, Y., C. C. Wu, and L. C. Lee, A study of multiple X line reconnection at the dayside magnetopause, *Geophys. Res. Lett.*, *15*, 295, 1988.

Spreiter, J. R., A. L. Summers, and A. Y. Alksne, Hydromagnetic flow around the magnetosphere, *Planet. Space. Sci.*, *14*, 223, 1966.

Van Allen, J., M. N. Oliven, and R. A. Fliehler, Magnetic field in the Earth's polar magnetosphere to 21 R_E, *EOS Trans. AGU*, *55*, 1167, 1974.

Van Allen, J. A., and J. Adnan, Observed currents on the Earth's high-latitude magnetopause, *J. Geophys. Res.*, *97*, 6381, 1992.

Walker, R. J., T. Ogino, J. Raeder, and M. Ashour-Abdalla, A global magnetohydrodynamic simulation of the magnetosphere when the interplanetary magnetic field is southward: The onset of magnetotail reconnection, *J. Geophys. Res.*, *98*, 17235, 1993.

Watanabe, K., and T. Sato, Global simulation of the solar wind-magnetosphere interaction: The importance of its numerical validity, *J. Geophys. Res.*, *95*, 75, 1990.

Wu, C. C., The effects of northward IMF on the magnetosphere, *Geophys. Res. Lett.*, *12*, 839, 1985.

Wu, C. C., R. J. Walker, and, J. M. Dawson, A three-dimensional MHD model of the Earth's magnetosphere, *Geophys. Res. Lett.*, *8*, 523, 1981.

Zwan, B. J., and R. A. Wolf, Depletion of solar wind plasma near a planetary boundary, *J. Geophys. Res.*, *81*, 1636, 1976.

Maha Ashour-Abdalla, Jean Berchem, and Joachim Raeder, Institute of Geophysics and Planetary Physics, University of California, Los Angeles, CA 90095-1567.